Mechanism for the efficient abstraction of an adsorbate by Cs^+ scattering at hyperthermal energies

R. J. W. E. Lahaye and H. Kang*
School of Chemistry and Molecular Engineering, Seoul National University, Kwanak-gu, Seoul 151-742, Republic of Korea
(Received 6 September 2002; published 6 January 2003)

In a classical molecular dynamics computer simulation, a different abstraction mechanism is proposed for an efficient formation of ion-adsorbate products between an impinging Cs^+ ion and an adsorbate on the Pt(111) surface. The two essential steps in this abstraction mechanism are the initial energy release to the surface by the impinging Cs^+ without affecting the adsorbate, and subsequently in its outgoing trajectory pulling the adsorbate away from the surface, due to the ion-dipole attraction. This Eley-Rideal–type mechanism will dominate in reactive scattering from a surface physisorbed with small molecules.

DOI: 10.1103/PhysRevB.67.033401 PACS number(s): 79.20.Ap, 34.50.Dy, 79.20.Rf

Ion scattering from surfaces with hyperthermal energies (1–100 eV) has a number of unique characteristics. The scattered ions are an excellent probe for surface properties, since penetration into the substrate or surface damage is negligibly small. The ions are also an ultrafast probe because the residence time in the vicinity of the surface is merely a few hundred femtoseconds. The impinging projectile has sufficient kinetic energy to break chemical bonds at the surface adding interesting chemical properties to this type of ion scattering.

Along these lines, recent studies of reactive ion scattering (RIS) from surfaces have discovered a range of phenomena such as dissociation of molecular projectile ions[1–6] and transfer of charges, atoms, or groups between the projectile ion and the surface.[7–15] Of particular interest is the abstraction of atoms or molecular fragments from surfaces by the projectile ion, which may have relevance to surface characterization and modification. Abstraction reactions have been observed with molecular projectile ions scattering from self-assembled monolayers and hydrocarbon surfaces[8,9] as well as with the scattering of O^+ from oxidized Si(100),[14] NO^+ from O/Al(111),[15] and Cs^+ from various kinds of adsorbates.[10–12] Charge exchange between a projectile ion and a surface often alters the reactively scattered ion intensity, making it difficult to analyze RIS yields in terms of a collision dynamics model. The simplicity of the RIS process with Cs^+ projectiles lies in the fact that charge exchange is small and can be ignored,[10] since the ionization energy of Cs (3.89 eV) is smaller than the work-function values of most semiconductors and transition metals.

Early experiments have measured very low yields for the Cs^+-adsorbate formation with chemisorbed species.[10] The RIS mechanism was assumed to be an extension of collision induced desorption: in a two-step process, the projectile at first collides with the adsorbate causing desorption, followed by the formation of the ion-adsorbate product in the outgoing trajectory. More recently, much higher RIS yields have been observed for Cs^+ scattered from H_2O, O_2, and CO_2 physisorbed on Pt(111) (Refs. 16 and 17) and from ultrathin ice overlayers,[11,12] which cannot be explained by the earlier proposed two-step process. Apparently, quantitative-mechanistic models are lacking for these efficient RIS processes. In this context, we have studied the scattering dynamics of the ion-adsorbate formation process using a classical molecular dynamics computer simulation, by measuring the desorption and RIS cross sections. Present work illuminates the role of the ion-adsorbate attraction in the RIS and desorption dynamics, and introduces a different abstraction mechanism that explains the large RIS yields.

An elaborate explanation of the scattering model and the simulation code is provided elsewhere.[18,19] In brief, the substrate contains five layers of 15×10 Pt atoms with a nearest-neighbor bimodal Morse potential. The impinging Cs^+ ion interacts with the Pt substrate via a pairwise additive Born-Mayer repulsive potential and an image-charge potential with respect to the perpendicular distance to the surface, resulting in a well depth of 1 eV for the potential-energy surface. The adsorbate is a structureless atomic point particle, with a specific mass and binding energy, governed by a Morse potential with the surface atoms. Because Cs^+ is isoelectronic to Xe, the only possible driving force to the Cs^+-adsorbate formation is the ion-dipole attraction. The ion-adsorbate interaction is in the form of a Born-Mayer repulsive potential and an induced ion-dipole attraction that combine to a well depth of 0.5 eV at 2 Å separation.

The simulation code solves Newton's equations of motion by means of the Numerov-Verlet integration algorithm.[20] The substrate is thermalized at 100 K, before the projectile starts its trajectory at 8 Å above the surface with an incidence angle of 45°. Each trajectory randomly impacts within a surface area that is large enough for the desorption process. A trajectory calculation terminates when the projectile once again reaches a distance of 8 Å above the surface, and the energy balance in the system (velocities, potential energies, and rovibrational excitation) determines whether the adsorbate has desorbed and the ion-adsorbate product has been formed. For each dataset, about 25 000 trajectories are calculated.

We have chosen an adsorbate with a mass of 16 amu and three binding energies with the surface, representing physisorption ($E_b=0.25$ eV), chemisorption ($E_b=1.0$ eV), and an intermediate case of $E_b=0.5$ eV. Figure 1 shows the cross sections for the desorption and RIS, as a function of the incidence energy of the Cs^+. The desorption cross sections

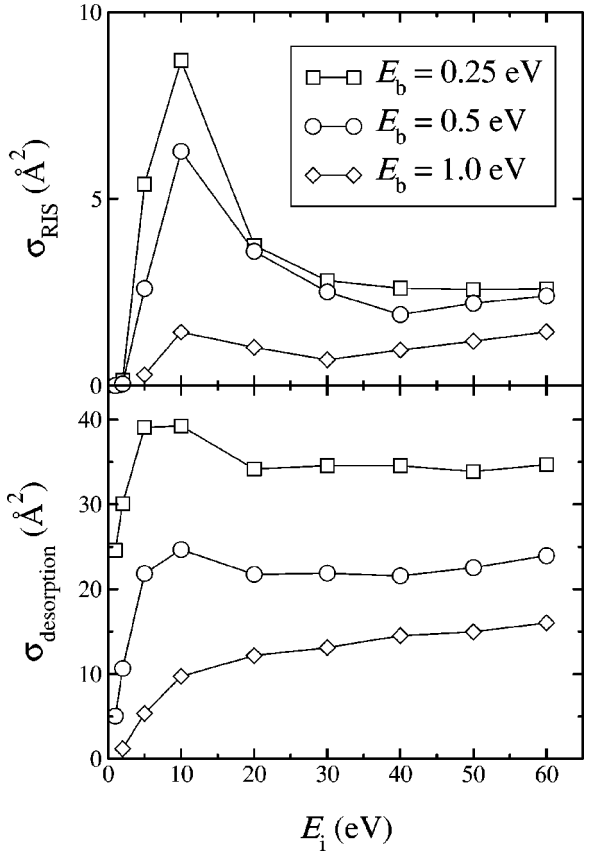

FIG. 1. Desorption and RIS cross sections for adsorbates of three binding energies E_b, as function of the incidence energy E_i of the Cs^+. The incidence angle of the Cs^+ is 45 and the adsorbate's mass is 16 amu.

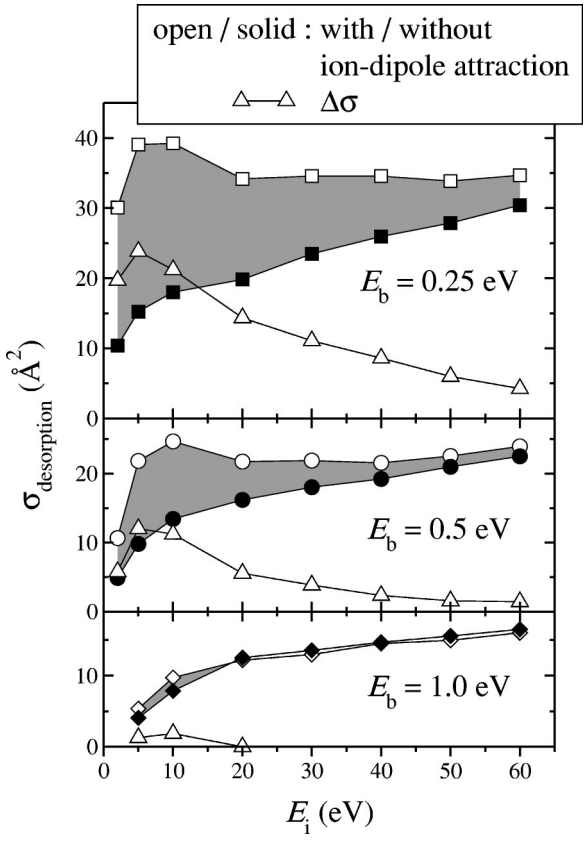

FIG. 2. Effect of the ion-dipole attraction on the desorption cross sections for an adsorbate of mass 16 amu and three binding energies E_b, as function of the incidence energy of the Cs^+. The Cs^+ ions impact the surface at an angle of 45°. Each panel shows the results for with and without the ion-dipole attractive potential, accompanied by the cross-section difference $\Delta\sigma$. The shaded areas indicate the enhancement to the desorption by the ion-dipole attraction.

show the typical energy dependence: a steep slope at low energy, reaching saturation as the incidence energy of the Cs^+ increases. Straightforward collision-induced desorption dynamics is sufficient to explain the steeper slope and a higher saturation value for a lower binding energy.[21–24] Rather unusual is the maximum at an incidence energy of $E_i = 10$ eV, observed only for the two lower binding energies of 0.25 and 0.5 eV. The corresponding RIS cross sections also show a similar slope and saturation with the increasing Cs^+ incidence energy, but where the desorption cross sections have a subtle maximum at $E_i = 10$ eV, the RIS cross sections show a distinct peak. Such a maximum in the desorption and RIS is absent in case of the stronger binding energy of $E_b = 1$ eV.

We have performed another similar set of simulations, but *without* the ion-dipole attractive potential, in order to examine the role of the attraction in the scattering dynamics. There is no RIS without the ion-dipole attraction and we only monitor the direct collision-induced desorption (CID) cross sections in this case. Figure 2 shows these CID cross sections together with the corresponding total desorption results from Fig. 1. The CID cross sections are always less, irrespective of the adsorbate's binding energy E_b. The shaded areas indicate the enhancement to the desorption by the ion-dipole attraction, which is also shown as the cross-section difference $\Delta\sigma$. The ion-dipole attraction contributes significantly for the two lowest binding energies of $E_b = 0.25$ eV and 0.5 eV, and the maximum at $E_i = 10$ eV is exclusively a result of the attraction between the Cs^+ and the adsorbate. The largest contribution to the desorption (i.e., the maximum in the $\Delta\sigma$ curve in Fig. 2) is in the low-energy range of the incidence Cs^+, where also the corresponding RIS cross sections in Fig. 1 have their maxima. The attractive force on the adsorbate by the Cs^+ is apparently most effective for low-energetic Cs^+ ions. The attraction contributes to the desorption only when the binding energy is similar to or smaller than the ion-adsorbate attraction of 0.5 eV; for $E_b = 1.0$ eV, the effect of the ion-dipole attraction is negligible.

Trajectory analysis shows that in the RIS process, the incidence Cs^+ initially collides with the surface without affecting the adsorbate, and subsequently in its outgoing trajectory pulls the adsorbate away from the surface. The impact must be in the vicinity of the adsorbate, so that the outgoing Cs^+ makes a close passage alongside of the adsorbate. This results in a high RIS efficiency only if the scattered Cs^+ is slow enough to give the attractive force sufficient time to accomplish the ion-adsorbate formation. For a successful

RIS process, it is crucial that the Cs^+ "misses" the adsorbate in its incoming trajectory, loses kinetic energy in the surface collision, and then drags the adsorbate along in its outgoing trajectory. The actual abstraction in the final step of this mechanism is only viable when the ion-dipole attractive force is strong enough to break the adsorbate's bond with the surface, which is feasible for weakly bound adsorbates.

The RIS process for chemisorbed species ($E_b = 1.0$ eV in Fig. 1) occurs through a mechanism different from the abstraction reaction. The projectile must collide directly with the adsorbate and transfer a sufficient amount of energy to break the 1.0 eV bond. Such a collision ought to be very precise because too much energy transfer will result in a velocity mismatch between the outgoing projectile and the adsorbate, which prevents the ion-adsorbate formation. Because this energy-transfer scheme is rather delicate, it is less probable. Hence, there are lower RIS cross sections for adsorbates with a stronger binding energy.

The crucial step in the RIS abstraction mechanism is the Cs^+ pulling the adsorbate away from the surface. For this to happen, the adsorbate's inertia needs to be overcome, since the adsorbate is accelerated from initially at rest to the velocity of the outgoing Cs^+ ion. This implies a mass dependence of the desorption and the RIS cross sections, which is shown for three adsorbate's masses in Fig. 3. The desorption cross sections are again calculated for with and without the ion-dipole attraction. Notice that the mass dependence almost vanishes when the ion-dipole attraction is absent (solid symbols in the lower panel of Fig. 3). In this case, the desorption occurs merely via a direct CID, which has no mass dependence as long as the projectile is much heavier than the adsorbate. The mass dependence arises when the attractive ion-dipole potential is included. The lower the mass, the greater the enhancement to the desorption cross sections and the higher the RIS cross sections. The lowest mass of 8 amu allows an enhancement of the desorption by the ion-dipole attraction for incidence energies up to 40 eV. However, for 32 amu, the enhancement has become very small and is also restricted to the incidence energy region below 15 eV.

The adsorbate's mass dependence and its variation with incidence energy E_i, as observed in Fig. 3, is an immediate result from the fact that the inertia of a lighter adsorbate has a lower resistance to following and attaching itself to the outgoing ion. Wherever the high-energetic outgoing Cs^+ is able to abstract a light adsorbate, the inertia of a heavier adsorbate would prevent it. Each adsorbate's mass has thus a maximum Cs^+ kinetic energy, above which the abstraction cannot take place anymore. This maximum kinetic energy for

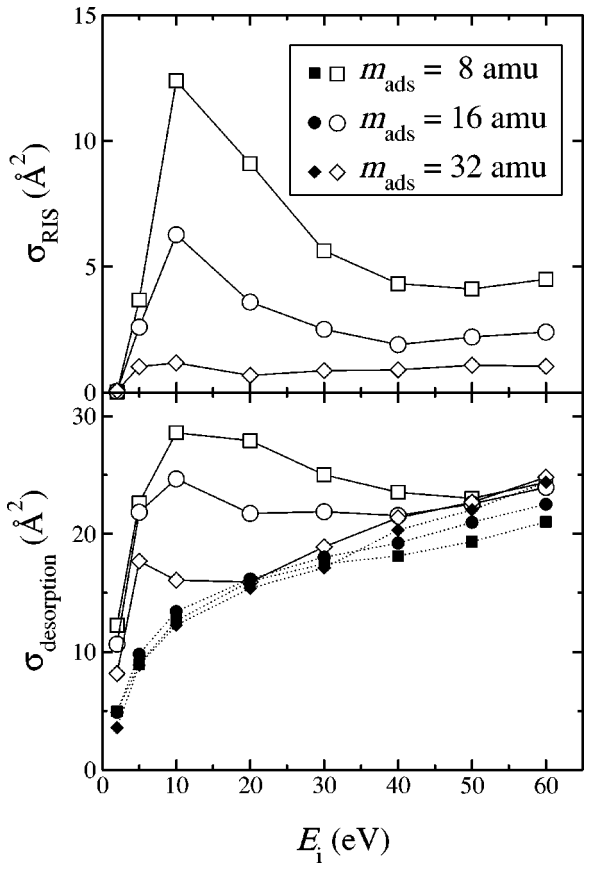

FIG. 3. Desorption and RIS cross sections for adsorbates of three masses with a binding energy E_b of 0.5 eV, as function of the incidence energy of the Cs^+. The Cs^+ incidence angle is 45°. The open and solid symbols in the lower panel represent with and without the ion-dipole attractive potential, respectively.

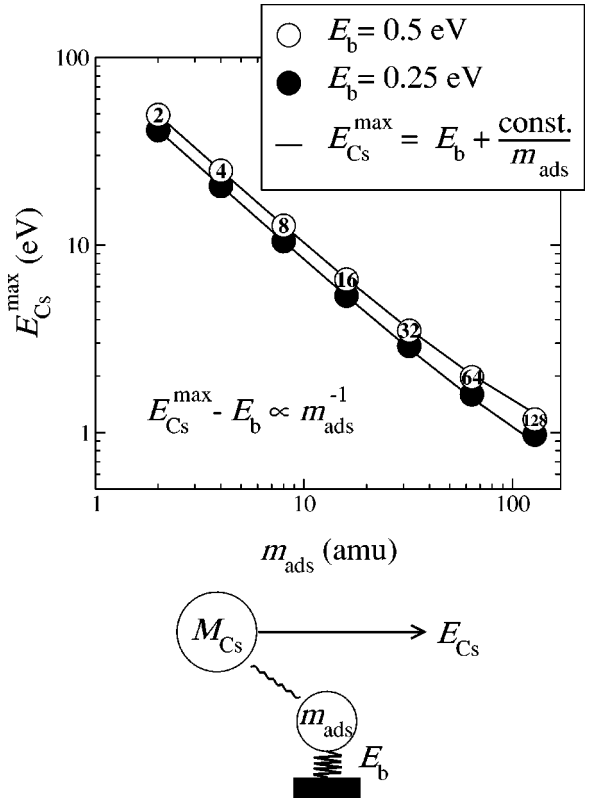

FIG. 4. Relation between the adsorbate's mass and the maximum kinetic energy of the Cs^+ for the abstraction mechanism. The adsorbate interacts in a two-dimensional model with the Cs^+ via the ion-dipole potential and is attached to the solid by a Morse potential with a well depth of E_b. The maximum Cs^+ energy for abstraction scales with m_{ads}^{-1} due to the inertia. The numbers in the open circles refer to the corresponding mass. Note that both axes use a logarithmic scale.

abstraction decreases with increasing mass. A two-dimensional abstraction model can illustrate this effect (see the reaction at the bottom of Fig. 4). A Morse potential with appropriate binding energy connects the adsorbate to a solid of infinite mass and the Cs^+ passes along the adsorbate in a straight line while interacting via the ion-dipole attractive potential. The maximum energy of the Cs^+ that is still able to drag the adsorbate along with it, E_{Cs}^{max}, is calculated for a number of adsorbate's masses, ranging from 2 to 128 amu. Figure 4 shows clearly in a logarithmic plot that E_{Cs}^{max} scales with m_{ads}^{-1}. Especially, the energy region between 5 and 20 eV is important because it covers the typical energies of the outgoing Cs^+. Therefore, the abstraction mechanism is most sensitive to adsorbates with a mass below 32 amu.

The mass effect in Fig. 4 does not depend much on the binding energy E_b, since the two curves almost overlap. Though the figure illustrates the importance of the adsorbate's inertia on the abstraction mechanism, this alone is not a measure for RIS. The RIS efficiency is the sum over the RIS probabilities of all kinetic energies of the outgoing Cs^+ up to the maximum kinetic energy as shown in Fig. 4. The result of this sum does depend on the adsorbate's binding energy in the way we have observed in Fig. 1.

The energy and angular distributions of the outgoing Cs^+-adsorbate product follow closely that of the attached Cs^+, owing to its much heavier mass. As a result, the abstraction mechanism has the following characteristics: (1) the angular distribution of the product follows the outgoing Cs^+, which is generally not centered along the surface normal, (2) the outgoing RIS product has a nonthermal energy distribution, and (3) no scaling with the energy of the incoming Cs^+ ions, because only the slow enough outgoing Cs^+ successfully abstracts the adsorbate. We consider the abstraction mechanism for RIS to be an Eley-Rideal process,[14,15,25,26] assuming that scaling with the incidence energy is not a requirement.

The simulation results predict almost an order of magnitude increase of the RIS cross sections when the abstraction mechanism comes into full swing (see the RIS peaks in Figs. 1 and 3). In experiments, RIS showed an increase by a factor of about 50 from chemisorbed to physisorbed water.[10,17] A permanent dipole of the adsorbate is omitted in the simulations, but may account for the somewhat larger RIS yields in the experiments. Nevertheless, the agreement between simulations and experiments is reasonable, indicating that the model contains the essential physics of the RIS process.

In summary, we have demonstrated an efficient RIS process occurring through an ion-adsorbate abstraction mechanism, in which a direct collision between the projectile and the adsorbate needs to be avoided. The abstraction efficiency depends on the velocity of the outgoing Cs^+ ions, and the adsorbate's mass and binding energy. Favorable conditions can be met for incidence energies of around 10 eV and for physisorbed adsorbates with a mass below 32 amu. Applications of such an efficient RIS process will be many, including surface analysis of soft molecular solids, such as ice. The scattering kinematics leading to abstraction should be relevant to other reactive projectiles as well.

We thank Professor Sangyoub Lee of the Theoretical Chemistry Lab for providing access to a cluster of eight 800 MHz Linux PCs. Financial support from the BK21 program by the Korean Ministry of Education is gratefully acknowledged.

*Electronic address: surfion@snu.ac.kr

[1] S.R. Kasi, H. Kang, C.S. Sass, and J.W. Rabalais, Surf. Sci. Rep. **10**, 1 (1989).
[2] H. Akazawa and Y. Murata, J. Chem. Phys. **92**, 5560 (1990).
[3] J.N. Greeley, J.S. Martin, J.R. Morris, and D.C. Jacobs, J. Chem. Phys. **102**, 4996 (1995).
[4] W.R. Koppers, J.H.M. Beijersbergen, T.L. Weeding, P.G. Kistemaker, and A.W. Kleyn, J. Chem. Phys. **107**, 10 736 (1997).
[5] S.A. Miller, H. Luo, S.J. Pachuta, and R.G. Cooks, Science **275**, 1447 (1997).
[6] D.G. Schultz and L. Hanley, J. Chem. Phys. **109**, 10 976 (1998).
[7] P. Haochang, T.C.M. Horn, and A.W. Kleyn, Phys. Rev. Lett. **57**, 3035 (1986).
[8] Q. Wu and L. Hanley, J. Phys. Chem. **97**, 2677 (1993).
[9] R.G. Cooks, T. Ast, T. Pradeep, and V. Wysocki, Acc. Chem. Res. **27**, 316 (1994), and references therein.
[10] M.C. Yang, C.H. Hwang, and H. Kang, J. Chem. Phys. **107**, 2611 (1997).
[11] T.H. Shin, S.-J. Han, and H. Kang, Nucl. Instrum. Methods Phys. Res. B **157**, 191 (1999).
[12] S.-C. Park, K.-W. Maeng, T. Pradeep, and H. Kang, Angew. Chem. Int. Ed. Engl. **40**, 1497 (2001), and references therein.
[13] R. Souda, T. Suzuki, H. Kawanowa, and E. Asari, J. Chem. Phys. **110**, 2226 (1999).
[14] C.L. Quinteros, T. Tzvetkov, and D.C. Jacobs, J. Chem. Phys. **113**, 5119 (2000).
[15] M. Maazouz, T.L.O. Barstis, P.L. Maazouz, and D.C. Jacobs, Phys. Rev. Lett. **84**, 1331 (2000).
[16] S.-J. Han, C.-W. Lee, H. Yoon, and H. Kang, J. Chem. Phys. **116**, 2684 (2001).
[17] J.R. Hahn, C.W. Lee, S.-J. Han, R.J.W.E. Lahaye, and H. Kang, J. Phys. Chem. A **106**, 9827 (2002).
[18] R.J.W.E. Lahaye, A.W. Kleyn, S. Stolte, and S. Holloway, Surf. Sci. **338**, 169 (1995).
[19] R.J.W.E. Lahaye and H. Kang, Surf. Sci. **490**, 327 (2001).
[20] M.P. Allen and D.J. Tildesley, *Computer Simulation of Liquids* (Oxford University Press, New York, 1987).
[21] R. Behrisch, *Sputtering by Particle Bombardment I* (Springer-Verlag, Berlin, 1981).
[22] L. Romm and M. Asscher, J. Chem. Phys. **110**, 3153 (1999).
[23] D. Kulginov, M. Persson, and C.T. Rettner, J. Chem. Phys. **106**, 3370 (1997).
[24] D. Velic and R.J. Levis, Surf. Sci. **396**, 327 (1998).
[25] E.W. Kuipers, A. Vardi, A. Danon, and A. Amirav, Phys. Rev. Lett. **66**, 116 (1991).
[26] C.T. Rettner, Phys. Rev. Lett. **69**, 383 (1992).